

## Article

# A Feasibility Study of a Respiratory Rate Measurement System Using Wearable MOx Sensors

Mitsuhiro Fukuda<sup>1</sup>, Jaakko Hyry<sup>1</sup> , Ryosuke Omoto<sup>1</sup>, Takunori Shimazaki<sup>2</sup> , Takumi Kobayashi<sup>1</sup> and Daisuke Anzai<sup>1,\*</sup> 

<sup>1</sup> Graduate School of Engineering, Nagoya Institute of Technology, Nagoya 466-8555, Japan

<sup>2</sup> Department of Clinical Engineering, Faculty of Health Care Sciences, Jikei University of Health Care Sciences, Osaka 532-0003, Japan

\* Correspondence: anzai@nitech.ac.jp; Tel.: +81-52-735-5389

**Abstract:** Accurately obtaining a patient's respiratory rate is crucial for promptly identifying any sudden changes in their condition during emergencies. Typically, the respiratory rate is assessed through a combination of impedance change measurements and electrocardiography (ECG). However, impedance measurements are prone to interference from body movements. Conversely, a capnometer coupled with a ventilator offers a method of measuring the respiratory rate that is unaffected by body movements. However, capnometers are mainly used to evaluate respiration when using a ventilator or an Ambu bag by measuring the CO<sub>2</sub> concentration at the breathing circuit, and they are not used only to measure the respiratory rate. Furthermore, capnometers are not suitable as wearable devices because they require intubation or a mask that covers the nose and mouth to prevent air leaks during the measurement. In this study, we developed a reliable system for measuring the respiratory rate utilizing a small wearable MOx sensor that is unaffected by body movements and not connected to the breathing circuit. Subsequently, we conducted experimental assessments to gauge the accuracy of the rate estimation achieved by the system. In order to avoid the effects of abnormal states on the estimation accuracy, we also evaluated the classification performance for distinguishing between normal and abnormal respiration using a one-class SVM-based approach. The developed system achieved 80% for both true positive and true negative rates. Our experimental findings reveal that the respiratory rate can be precisely determined without being influenced by body movements.

**Keywords:** respiratory rate; MOx sensor; eCO<sub>2</sub>; wearable device



**Citation:** Fukuda, M.; Hyry, J.; Omoto, R.; Shimazaki, T.; Kobayashi, T.; Anzai, D. A Feasibility Study of a Respiratory Rate Measurement System Using Wearable MOx Sensors. *Information* **2024**, *15*, 492. <https://doi.org/10.3390/info15080492>

Academic Editor: Luis Martínez López

Received: 8 July 2024

Revised: 7 August 2024

Accepted: 14 August 2024

Published: 16 August 2024



**Copyright:** © 2024 by the authors. Licensee MDPI, Basel, Switzerland. This article is an open access article distributed under the terms and conditions of the Creative Commons Attribution (CC BY) license (<https://creativecommons.org/licenses/by/4.0/>).

## 1. Introduction

The aging trend within Japan's population has been steadily advancing in recent years, posing challenges for managing the health of the elderly, as is particularly evident in evacuation centers during disasters [1–4]. This issue is exacerbated by the scarcity of healthcare personnel. In evacuation centers situated in sparsely populated regions, there is a growing need to remotely monitor the health conditions of the elderly due to the limited availability of medical staff [5]. Monitoring devices equipped with wireless modules [6,7] have been proposed, which facilitate the acquisition and remote monitoring of vital signs like heart rate, body temperature, and SpO<sub>2</sub> using wearable technology [8]. From a medical standpoint, assessing an individual's breathing status is crucial for remote health management. In addition to SpO<sub>2</sub> values, factors such as breathing rhythm, depth, and frequency play a significant role in evaluating the respiratory status [9].

In general, methods for monitoring respiratory status are devised using thoracic impedance [10] in conjunction with an electrocardiogram (ECG) or a method for measuring the respiratory rate by analyzing pulse waves [11]. However, these methods are susceptible to interference from body movements, requiring the subject to remain still during the measurements. In clinical practice, capnometers [12,13], which measure CO<sub>2</sub>

concentrations from exhalation, are widely used for monitoring the respiratory status at the breathing circuit when using ventilators or Ambu bags. They can non-invasively measure the end-expiratory carbon dioxide gas partial pressure (the end tidal CO<sub>2</sub>), which is an approximation of the partial pressure of carbon dioxide gas. Although the respiratory rate can also be obtained at the same time, capnometers are not solely used to measure the respiratory rate, and the mouth needs to be covered with an oxygen mask to prevent gas leakage.

Previous studies have used a method where a belt was wrapped around the chest and the displacement of the thorax was measured with a strain gauge [14], a method to accurately estimate the respiratory rate by combining an electrocardiography with photoplethysmography [15], and a method using impedance pneumography, in which a weak high-frequency current was applied to the thorax to convert impedance changes to the respiratory rate [16]. However, these require wearing a belt and contact sensors on the skin, which are cumbersome and require hygiene considerations. Therefore, studies have been conducted to estimate the respiratory rate during walking and running based on breathing sounds recorded with a microphone [17], and in non-contact studies, using video cameras [18]. However, the use of microphones requires some privacy measures, as outside environmental noises or conversations may be inadvertently caught due to the microphone volume being more sensitive during lower breathing events, like during resting, compared to the level of the volume sensitivity during larger breathing events, like walking or running. Video cameras can also capture private, personal information from the surrounding areas. Furthermore, the sensors themselves are expensive and require advanced processing, making them difficult to produce at low cost.

There are two types of CO<sub>2</sub> sensors: non-dispersive infrared (NDIR) and Fourier-transform infrared spectroscopy (FTIR), of which NDIR is used in studies of exhaled gas management [19]. However, this method requires an optical path of a certain length between the light-emitting and light-receiving parts, which makes it difficult for the sensor to be compact and wearable. The FTIR method also uses infrared light as the source, the interference of light using beam splitters, and mirrors to measure the concentration. The beam splitters and mirrors are large and not suitable for wearing. With these limitations, it is difficult to make a wearable CO<sub>2</sub> sensor. This study proposes a method to measure the respiratory rate using an eCO<sub>2</sub> with an MOx sensor, for the development of a wearable, non-contact device at a low cost.

As a background, a previous study [6] focused on wearable monitoring systems that can, for example, gather vital data via wireless communication. With these systems, multiple kinds of sensors, including thermopile, humidity, and ECG, are wirelessly connected, and all measured data are gathered in a cloud server. Subsequently, a machine learning method is applicable for detecting the heat strain status, for example. In our study, based on the concept of wireless monitoring systems, we tried to measure the respiratory rate with our device and create remote monitoring capabilities for the measurements. In addition, machine learning methods can be applied for classifying between normal and abnormal breathing, which should contribute to the improvement in the accuracy of the system.

While previous research has attempted to analyze the CO<sub>2</sub> concentration from an eCO<sub>2</sub>, the novelty of this study is in the detection of the respiration rate. This study focuses on tracking the changes in CO<sub>2</sub> levels and investigates the possibility of continuous monitoring of the respiratory rate status in the CO<sub>2</sub> levels using compact wearable eCO<sub>2</sub> sensors, which can be designed to be small and resistant to artifacts produced from body movements. The target is a method to estimate the normal breathing pattern while also accounting for abnormal breathing events, such as coughing and yawning, as well as body movement artifacts. In particular, we examined the potential of using a wearable metal oxide (MOx) sensor indoors. These sensors are very reliable, highly cost-effective, and designed to detect volatile organic compounds (VOCs). The sensor used in this study has been shown to be suitable for indoor use and has good correlation with other MOx sensors capable of measuring eCO<sub>2</sub> levels [20]. While MOx sensors do not directly measure CO<sub>2</sub>

levels, they can estimate the equivalent  $\text{CO}_2$  concentration (namely,  $e\text{CO}_2$ ) using linear transformation based on the total VOC (TVOC) concentration, where the proportional constant is the additive constant ranging at around 400 vol.-ppm  $\text{CO}_2$  in pollutant-free outdoor air, and the bias is the factor between exhaled  $\text{CO}_2$  and TVOCs. The simplest form of this relationship can be described using the following equation:

$$c(\text{CO}_2) = a + b \cdot c(\text{TVOC}) \quad (1)$$

where  $c(\text{CO}_2)$  is the  $\text{CO}_2$  concentration,  $c(\text{TVOC})$  is the TVOC concentration,  $a$  is the additive constant ranging at around 400 vol.-ppm  $\text{CO}_2$  in pollutant-free outdoor air, and  $b$  is the factor between the exhaled  $\text{CO}_2$  and the TVOCs, as stated in [21].

In the developed system, we placed the sensor on a medical mouth shield that was commonly used during the COVID-19 pandemic. This commonly available mouth shield is produced by Virec (Model NK-002) and has a convenient shape and size. Considering real-world scenarios, the effects of sleeping and other physical movements, as well as the feasibility of detection and removal by filtering out coughing and yawning variables, were investigated through an experimental evaluation. In a related experiment [22], it was shown that a mouth shield is not necessarily needed when indoors; however, if used while walking and running indoors and when moving outdoors, it may be needed due to wind or airflow affecting the measurements. If a mouth shield is not used, the sensor is attached in front of the mouth or under the nose. This can be performed, for example, by using a flexible plastic frame to fix the sensor in front of the mouth or under the nose.

Additionally, we developed a normal respiration rate detection method based on a one-class support vector machine (SVM) because coughing and yawning strongly affect the accuracy of respiration rate estimation. The purpose of SVM here is to determine whether the respiration is normal or abnormal and to only measure the normal respiration from the respiration rate. The developed detection system tries to distinguish the coughing and yawning states as outlier respiration to establish the respiratory rate estimation only in the normal states. We applied the short-term Fourier transform technique to the measured  $e\text{CO}_2$  data for analysis of the time variation of each frequency component. Then, the short-term Fourier transform results were employed for the one-class SVM algorithm as learning data. We also carried out an experiment to evaluate the performance of the developed one-class SVM-based system. Finally, the performance evaluation results are demonstrated and discussed to determine if the respiration rate measurement method is reliable.

## 2. Materials and Methods

### 2.1. $\text{MO}_x$ Sensor

$\text{MO}_x$  sensors (metal oxide sensors) are used for measuring changes in the resistance of metal oxides, such as tin oxide ( $\text{SnO}_2$ ) and zinc oxide ( $\text{ZnO}$ ), caused by  $\text{H}_2$  molecules and volatile organic compounds (VOCs). Figure 1 shows the process where the sensor is heated to more than 200 degrees, and the electrons on the surface of the metal oxide are lost between the electrons and the oxygen molecules. This ionizes the oxygen ( $\text{O}_2$ ) adsorbed on the surface of the metal oxide, thus forming negative oxygen ions ( $\text{O}_2^-$ ).

When gases come into contact with the surface of the sensor, these gas molecules react with the oxygen ions on the surface of the metal oxide. This chemical reaction causes the oxygen ions to take electrons from the gas molecules and return them to the metal oxide. The resulting electron transfer makes the metal oxide conductive and changes the resistance of the sensor.  $e\text{CO}_2$  is calculated as the equivalent carbon dioxide concentration based on the resistance value change based on the  $\text{H}_2$  concentration.

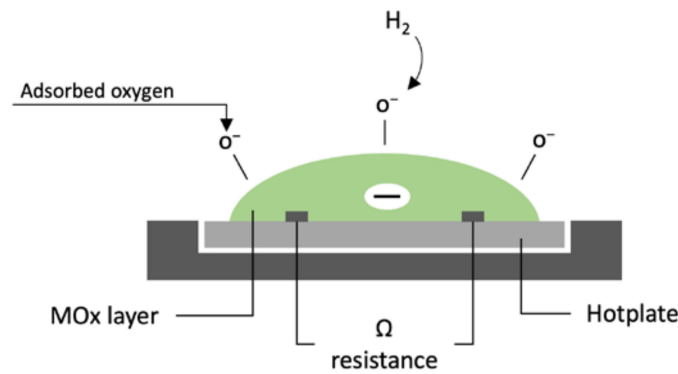


**Figure 1.** MOx sensor working principle, where oxygen is adsorbed onto the surface of the metal oxide.

We used a MOx sensor CCS811 (from ams OSRAM, Premstaetten, Austria) with a high sampling rate and low power consumption as the eCO<sub>2</sub> sensor. The advantages of the device are miniaturization and real-time performance, as the sensor size is only 3 mm × 3 mm. The power consumption is approximately 1 mW to 46 mW, so, assuming that the design has a low power consumption mode, we believe that the sensor can be operated with a small battery. We can estimate the power consumption, including the micro-hotplate, as follows. Assuming a small battery of 500 mAh, intermittent operation with a duty ratio of 10% (i.e., working for 0.1 s during a 1 s period), and, additionally, that the main power consumption arises from the use of the MOx sensor and the microcomputer (Arduino, Monza, Italy), the final achievable lifetime (operating time per charge) would be more than 150 h. This micro-hotplate-technology-based smart sensor also has a gas sensor for detecting low concentrations of volatile organic compounds (VOCs), which are mainly detected indoors with a microcomputer and an analog-to-digital (A/D) converter. An example of the MOx sensor and the circuit configuration of the CCS811 used in this study are shown in Figure 2. This configuration detects ethanol, organic compounds (VOCs), and total volatile organic compounds (TVOCs) and outputs digital values of the sensor results via an I2C interface. When a person generates VOCs, the equivalent level of CO<sub>2</sub> (eCO<sub>2</sub>) can be detected [23]. Figure 3 shows an example of the measured eCO<sub>2</sub> concentrations using the CCS811 sensor (the experimental setup is described in Section 2.2). The results confirm the eCO<sub>2</sub> concentration peaks during breathing and that the wearable MOx sensor utilized in this study operates properly for breathing rate detection. For the filtering of respiration data with machine learning, the sensor is connected from a wireless network to a cloud server, where data processing is performed.

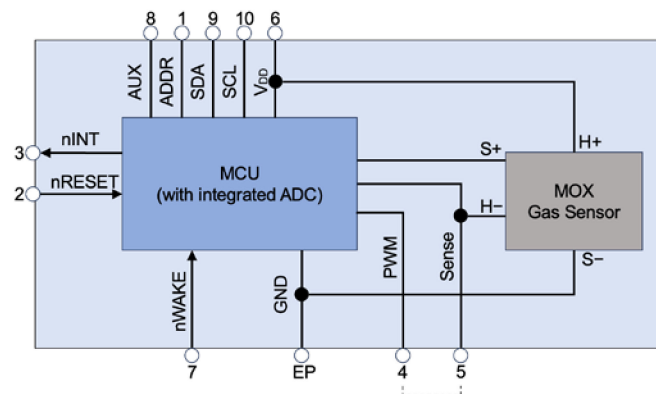


**Figure 2.** Circuit configuration of the wearable MOx sensor for detecting (eCO<sub>2</sub>) from the VOC and TVOC levels.

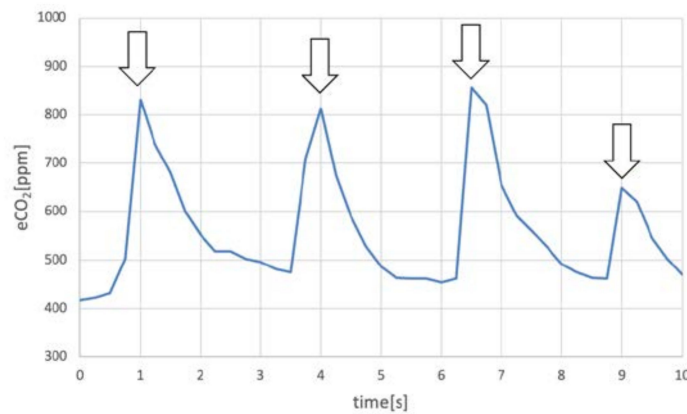


**Figure 3.** Measured waveforms of the wearable MOx sensor, showing the eCO<sub>2</sub> concentration peaks (indicated by the arrows).

2.2. Experimental Measurement Environment

Figure 4a shows the experimental measurement environment. The eCO<sub>2</sub> concentrations were measured in both the supine and lateral positions of the examinee using the sensor in a mouth shield, as shown in Figure 4b. In addition, a 16 s period of apnea was created immediately before the measurement started to stabilize the internal condition of the wearable MOx sensor before commencing the eCO<sub>2</sub> concentration measurement. Figure 4c shows the equipment configuration where the sensor and MCU were incorporated into a mouth shield, connected to a microcomputer and a laptop PC. Table 1 shows the details of the exact laboratory equipment used in the measurement experiments, including the wearable MOx sensor.

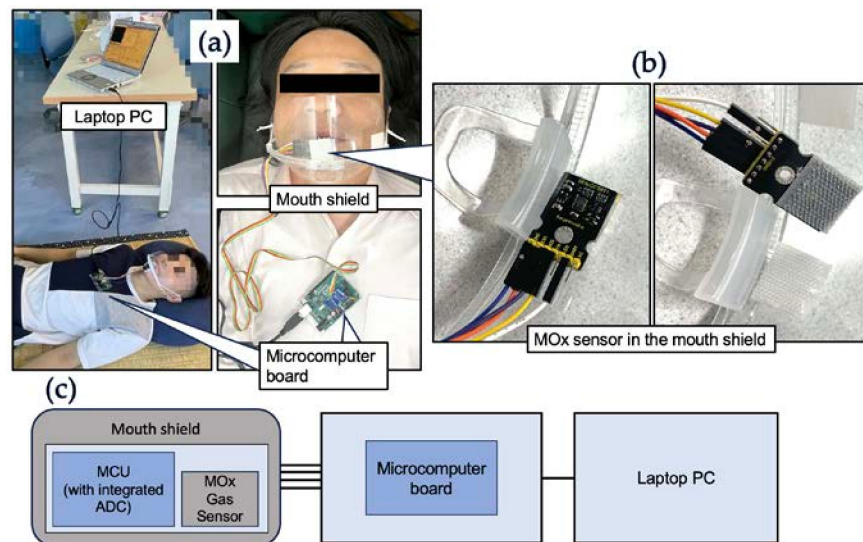


**Figure 4.** Experimental environment: (a) physical setup overview, (b) attachment of the wearable MOx sensor in the mouth shield, and (c) equipment configuration diagram.

**Table 1.** Details of experimental equipment.

Parts	Part Name & Manufacturer Origin
MOx sensor	KS0457 keystudio CCS811 Carbon Dioxide Air Quality Sensor, Shenzhen, China
Microcomputer board	Arduino UNO A000066, Monza, Italy
Mouth shield	Virec NK-002, Saitama, Japan
Pillow	Polyester cushion, Tokyo, Japan

### 2.3. Evaluation Method of Wearable MOx Sensor

The sampling rate of the wearable MOx sensor was set to the maximum possible frequency of 4 Hz for the CCS881 device. Estimation of the respiratory rate was carried out under two conditions: (1) at rest and turning over to simulate body movement, and (2) at rest while coughing and yawning. In this environment, the eCO<sub>2</sub> concentration was measured, and the respiratory rate was estimated by detecting peaks using the thresholds obtained from the results. Peak detection was performed on the concentration time waveform. The respiratory rate  $R$  (bpm) in this study was calculated using the following formula:

$$R = \frac{N_r}{T} \quad (2)$$

where  $N_r$  and  $T$  are the number of breaths detected and the measurement time (min), respectively. As a reference value for comparing with the estimated respiratory rate, a metronome was used to ensure that the subject's actual breathing rate was 22.5 bpm. In this experiment, we set the target for normal breathing as 22.5 bpm, as this is at the center of a typical breathing rate, which is roughly a single breath per three seconds. A normal breathing rate is commonly assumed to be between 5 bpm to 40 bpm. The threshold in this study was determined by the maximum value of the eCO<sub>2</sub> concentration  $c$ . The threshold  $t$  can be calculated as  $t = \alpha \cdot c$ , where the  $\alpha$  is optimally selected between 0.4 and 0.6. It is noted that the optimal coefficient  $\alpha$  varies in each subject, so we need to set the optimal value for each subject to achieve an accurate respiratory rate. To improve the sensitivity, we set a bandpass filter to cover ranges from 16.5 to 28.5 bpm to suppress the superimposed noises. In this study, one inhale and exhale were counted as one breath. Since the main frequency component of the eCO<sub>2</sub> concentration waveform data obtained from the MOx sensor should be 22.5 bpm (=0.375 Hz), bandpass filtering with a low-frequency cut-off frequency of 0.275 Hz and a high-frequency cut-off frequency of 0.475 Hz were applied to the measured data. This was performed to reduce the effect of CO<sub>2</sub> concentration changes not related to respiration. The maximum normalized filter output exceeded a threshold value of 0.369, which was then counted as one breath, and the subject's breathing rate was estimated. The threshold was calculated based on the normalized filter output with a coefficient of around 0.4. The validity of the breathing rate estimation with the wearable MOx sensor was verified by comparing the estimated breathing rate with the subject's actual breathing rate of 22.5 bpm. The respiratory measurement was performed using the peak detection algorithm, which requires an appropriate threshold. Factors like coughing affect the time-domain waveforms of the eCO<sub>2</sub> concentration, so the optimal threshold is the difference between normal and abnormal respiration.

### 2.4. Experiment 1: Measurement at Rest and during Body Movement

The breathing states of eight adult males during rest in a supine position were measured, including six nasal breaths and six oral breaths. Subsequently, in the same position, six breaths were measured using nasal breathing and six using mouth breathing, while transitioning between the left and right lateral decubitus positions to verify the effect of body movements.

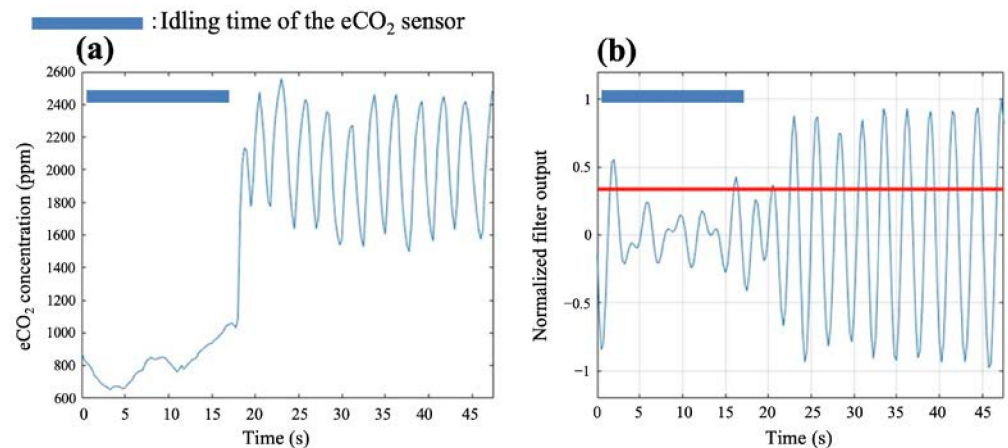
### 2.5. Experiment 2: Measurement with Coughing and Yawning

As in Experiment 1, the respiratory states of eight male adults at rest in a supine position were measured for a total of 12 breaths, including both nasal and mouth breathing. This was followed by coughing and yawning, and each action was repeated 12 times for a total of 15.96 s. The effect of coughing and yawning on the respiratory rate was verified from the obtained eCO<sub>2</sub> concentration waveform.

## 3. Experiment Results and Discussion

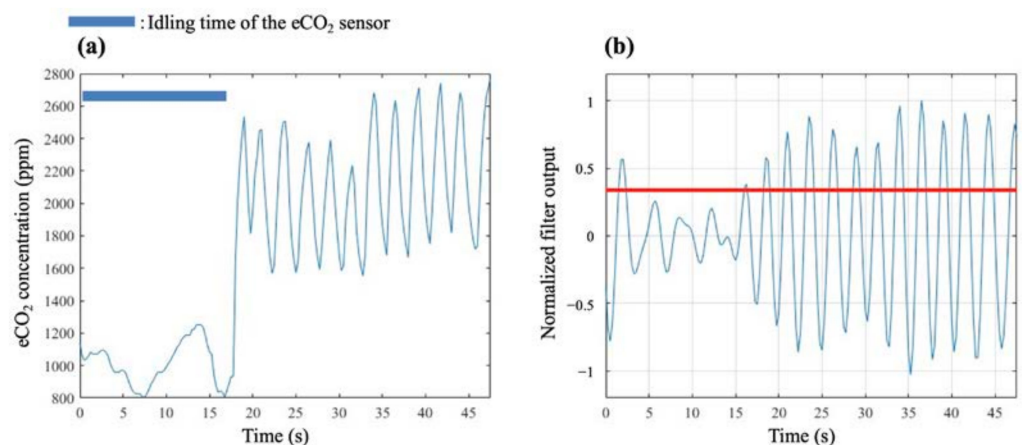
Figure 5a shows an example of a time waveform of the eCO<sub>2</sub> concentration at rest, as obtained from this experiment. The results in this figure show a sharp peak that

corresponds to the subject's breathing, indicating the possibility of estimating a respiratory rate. Figure 5b shows the time waveform of a normalized filter output when using bandpass filtering for the measured data of the subject's eCO<sub>2</sub> concentration. We used two process steps: one was bandpass filtering, and the other was normalization. The bandpass filtering had a low-frequency cut-off frequency of 0.275 Hz and a high-frequency cut-off frequency of 0.475 Hz, which were applied to the measured data. Then, normalization was adapted, where the maximum value was normalized to 1. Because of the bandpass filtering, the DC component could be removed. The appropriate threshold shown in red indicates that the subject's respiratory rate could be estimated.



**Figure 5.** Experimental results at rest: (a) eCO<sub>2</sub> concentrations and (b) normalized filter output, where the idling time of the eCO<sub>2</sub> sensor is indicated with the blue bar.

Figure 6a,b show the time waveforms of the eCO<sub>2</sub> concentration when body motion was introduced and the resulting output waveforms of the normalized bandpass filters, respectively. In terms of both the comparison of the time waveforms of the eCO<sub>2</sub> concentrations in Figures 5a and 6a and comparing the filter outputs in Figures 5b and 6b, no significant differences were found in the results obtained at rest and during body movement that would affect estimation accuracy. It was also found that the system was able to detect the concentrations of eCO<sub>2</sub> without being affected by body movements, and it enabled estimation of the respiratory rate.



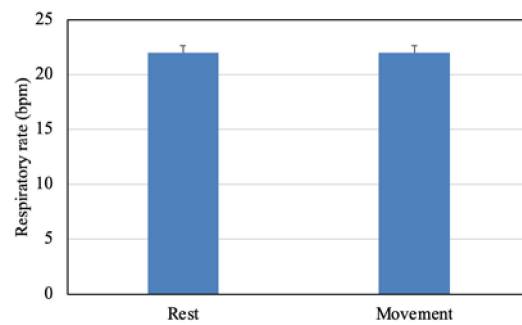
**Figure 6.** Experimental results of time waveforms for eCO<sub>2</sub> concentration during body movement: (a) eCO<sub>2</sub> concentrations and (b) normalized filter output.

Table 2 and Figure 7 show the mean values and standard deviation results for the eight subjects measured both at rest and during body movement. For the reference value

of 22.5 bpm in the experiment, an average estimate of 22.03 bpm was achieved, and an absolute error of 0.47 bpm was obtained with good estimation accuracy. In addition, a standard deviation of 1.555 bpm was observed, and it was confirmed that the standard deviation of the change due to individual differences was relatively small, at less than 2 bpm. There were no significant changes in the means or standard deviations of the estimated respiratory rates for the eight subjects at rest or in body motion, indicating that the system was also highly unaffected by body movements.

**Table 2.** Estimated respiratory rate statistics at rest and during movement.

	Average	Standard Deviation
Rest	22.03 bpm	1.555 bpm
Movement	22.03 bpm	1.555 bpm



**Figure 7.** Comparison of the estimated respiratory rates at rest and during body movement.

The next step was to investigate the effects of coughing and yawning on measuring eCO<sub>2</sub> levels at rest. Figure 8a shows the measured waveform of the eCO<sub>2</sub> concentration with coughing and yawning. Here, 48 to 64 s was the time waveform of the eCO<sub>2</sub> concentration measured with coughing, and 64 to 80 s was the time waveform of the eCO<sub>2</sub> concentration measured with yawning. In the waveform of the measured eCO<sub>2</sub> concentration, the presence of coughing and yawning resulted in a superimposition of different frequency components. It can also be observed that coughing had higher-frequency components than breathing, while yawning had lower-frequency components than breathing.

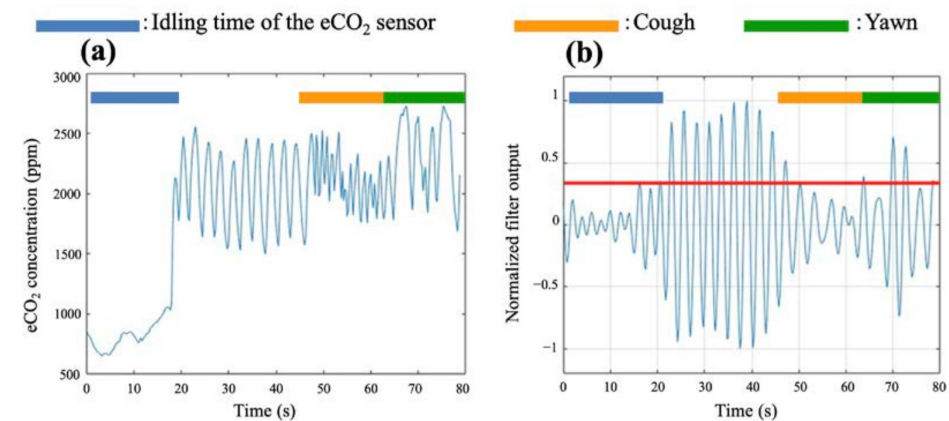


**Figure 8.** (a) eCO<sub>2</sub> concentration obtained in this experiment (cough, yawn), and (b) normalized filter output (cough, yawn), where the blue, orange, and yellow bars indicate the idling of the sensor, coughing, and yawning, respectively.

Figure 8b shows the time waveform after applying a bandpass filter to the measured eCO<sub>2</sub> concentration data during coughing and yawning. Since the eCO<sub>2</sub> changes caused

by coughing and yawning had frequencies close to respiration, the bandpass filters used in this experiment did not adequately eliminate these changes. In the filter output shown in Figure 8b, a peak value of at least 0.369 is present in the measured waveform of the eCO<sub>2</sub> due to deletion detected at around 70 s, which resulted in a false single breath detection. This suggests that depending on the type of yawn, a temporal waveform of yawning may occur that has components similar to the frequency characteristics of breathing.

Finally, Table 3 and Figure 9 show the means and standard deviations of the estimated respiratory rate with and without coughing and yawning conditions. The results show that coughing and yawning are influenced by the estimated accuracy of the breathing rate. The estimated mean breathing rate was 26.72 bpm, with an absolute error of 4.22 bpm compared to the reference value of 22.5 bpm.

**Table 3.** Estimated respiratory rate means and standard deviations with and without coughing and yawning.

	Average	Standard Deviation
w/o cough, yawn	22.03 bpm	1.555 bpm
w cough, yawn	26.72 bpm	2.043 bpm

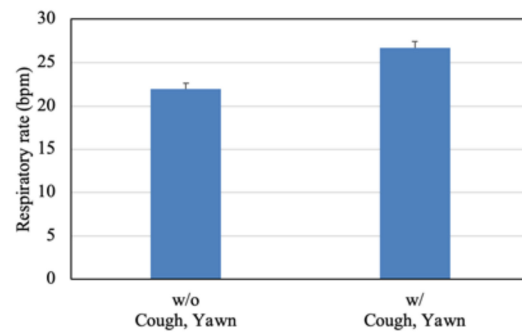


**Figure 9.** Comparison of the estimated respiratory rates for coughing and yawning.

#### 4. One-Class SVM-Based Normal Respiration Detection

##### 4.1. Principle

The support vector machine (SVM) is a machine learning algorithm that aims to find a hyperplane that maximally separates two different classes as a binary classification. Although SVM is commonly used as a supervised learning method for binary classification, this study employed a one-class SVM for outlier detection as an unsupervised learning method [24,25]. Let us define a vector ( $d \times 1$ )  $x$  as  $[x_1, x_2, \dots, x_d]^T$ , and the  $i$ -th vector  $x$  ( $1 \leq i \leq n$ ) is expressed by  $x^{(i)} = [x_1^{(i)}, x_2^{(i)}, \dots, x_d^{(i)}]^T$ . In the one-class SVM algorithm, feature extraction applies nonlinear transformation for mapping  $x$  to a higher dimension.

Here, we also define the feature vector ( $h \times 1$ ) as  $\phi(x) = [\phi_1(x), \phi_2(x), \dots, \phi_h(x)]^T$ , where  $\phi_j(x)$  ( $1 \leq j \leq h$ ) is a nonlinear function to extract the features of the vector  $x$ . The inner product of the feature vector  $\phi(x)$  and a parameter vector  $w$  ( $h \times 1$ ) is given by

$$f(x) = w^T \cdot \phi(x) \tag{3}$$

Note that the inner product  $f(x^{(i)})$  for  $x^{(i)}$  should be a scalar value. For outlier classification, we classify the data  $x^{(i)}$  into two clusters based on a positive threshold  $\rho$ . Taking into consideration that  $w$  corresponds to the direction of the feature vector  $\phi(x)$  if  $x$  is correct data (non-outlier data), the cluster of the correct data should concentrate around a certain value of  $f(x)$ . Furthermore, the inner product with  $w$  and the feature vector of the outlier data, which is orthogonal to that of the correct data, can be expected to have a value

close to 0. Therefore, outlier detection based on the one-class SVM can be performed with the following equations:

$$f(x^{(i)}) \geq \rho \quad (4)$$

$$f(x^{(i)}) < \rho. \quad (5)$$

Here, the data  $x^{(i)}$  can be classified as correct data when Equation (4) is satisfied. On the other hand, the data  $x^{(i)}$  that satisfy Equation (5) can be detected as outlier data.

The larger the dataset, the better it is able to account for human differences and to prevent over-training. However, in this study, data augmentation was used to increase the size of the dataset. Data augmentation was performed by adding AWGN from  $-10$  dB to  $10$  dB in  $0.1$  dB increments to the raw respiration data. Four normal respirations and four abnormal respirations were measured per person, and the data expansion increased the number of measurements by approximately 200-fold.

## 4.2. Performance Evaluation

### 4.2.1. Setup

To evaluate the accuracy of classification between normal and outlier respiration, the  $e\text{CO}_2$  concentration was measured using the MOx sensor used in the previous experiment. The MOx sensor was attached to the front of the subject's mouth. There were eight adult male subjects between the ages of 21 and 25 in the experiment. In each measurement, the  $e\text{CO}_2$  concentration was measured under apnea, nasal respiration, mouth respiration, coughing, and yawning situations at a rest state, and under apnea, nasal respiration, and mouth respiration situations during body movement. Of the eight subjects, six were assigned to training data and two to test data. Only normal breathing (nasal and mouth) was used for the training data, and both normal and abnormal breathing (apnea, cough, and absence of breath) were used for the test data. The SVM input was short-time Fourier transform (STFT) respiratory data, and the output of the SVM was a one-dimensional value, so the normality or abnormality was estimated using a threshold value. The closer the output is to the training data, which are normal respiration data, the larger the value of the output. After estimation was performed on all test data, the TNR, FPR, TPR, and FNR were obtained.

Figure 10 shows an example of the  $e\text{CO}_2$  measurement data at the rest state, where not only normal respiration but also outlier respiration was observed. The data were pre-processed for the removal of the DC component, interpolation on the time domain, and short-time Fourier transform (STFT). The STFT was used to analyze the time variation of the frequency components in the measured  $e\text{CO}_2$  concentration.

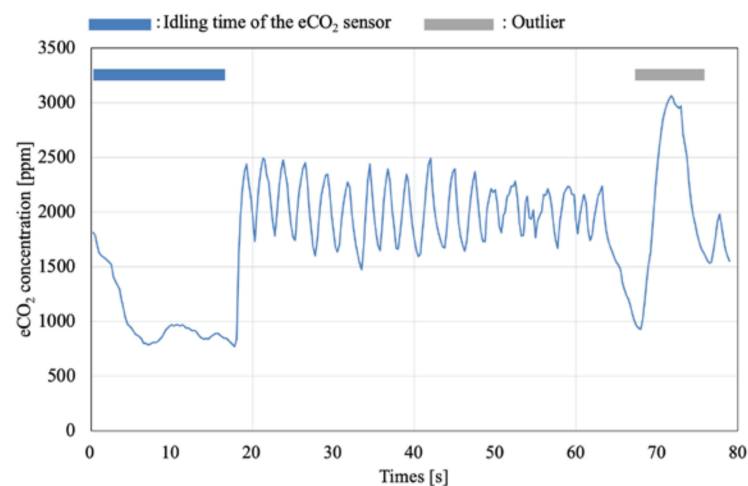
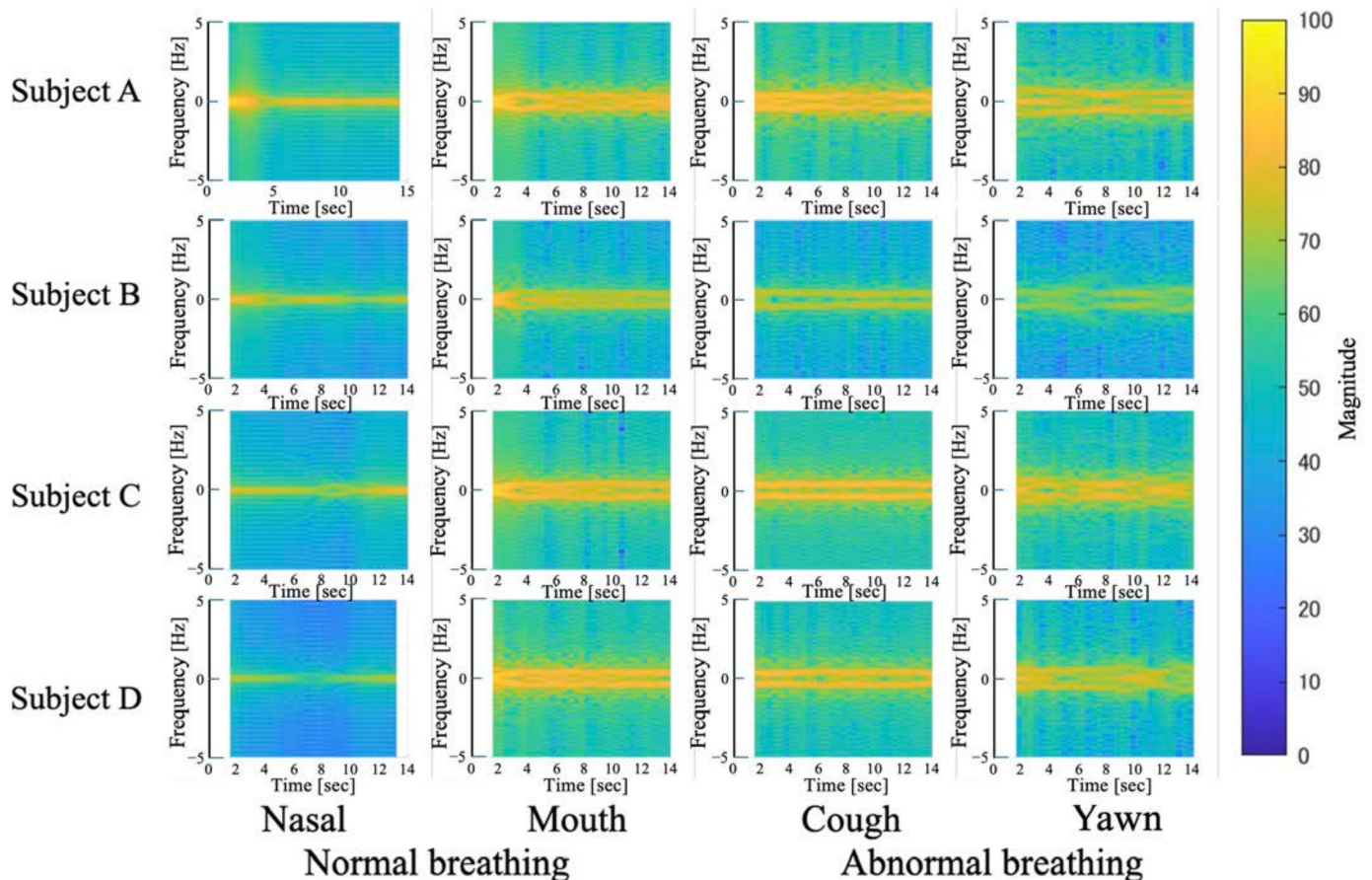


Figure 10.  $e\text{CO}_2$  concentration in a rest state with an observed outlier.

Figure 11 shows examples of the STFT for the measured data, where we can see that nasal breathing had a certain, narrower frequency component that was stronger and had less temporal variation. Mouth breathing had a wider frequency range than the nasal breathing, but the temporal variation was as small as the nasal breathing. On the other hand, abnormal breathing, depicted as coughs and yawns, had patterns that were characterized by a wider frequency range compared to normal breathing, while also having greater temporal variation.



**Figure 11.** Examples of short-time Fourier transform ( $-5$ – $5$  Hz) measurements, showing the differences in the nasal, mouth, cough, and yawn frequency characteristics.

Then, for evaluating the one-class SVM-based classification, two datasets (test and learning datasets) were randomly selected from all measurement data. The true negative rate (TNR), false positive rate (FPR), true positive rate (TPR), and false negative rate (FNR) were employed as the evaluation metrics.

#### 4.2.2. Results and Discussion

Figure 12 shows the changes in the estimation accuracy with respect to the threshold value  $\rho$ . All four evaluation metrics were sensitive to the threshold setting, so we should further optimize the threshold to achieve better performance. Additionally, Table 4 shows the confusion matrix when the threshold value was optimized for the TPR and TNR criteria. From these results, it can be confirmed that one-class SVM-based classification achieved a TNR and TPR of approximately 80% by appropriately selecting the threshold value.

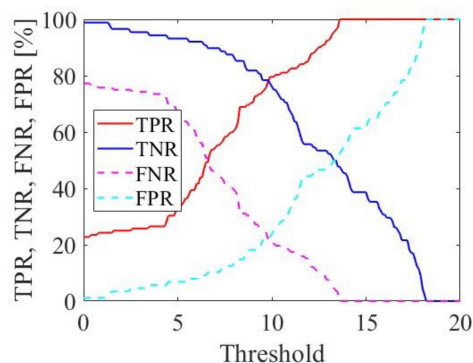


**Figure 12.** Changes in the estimation accuracy for true negative rate (TNR), false positive rate (FPR), true positive rate (TPR), and false negative rate (FNR).

**Table 4.** Confusion matrix (TPR, TNR, FNR, and FPR) showing true negative and true positive rates values achieving close to 80% % indicated by the red colour.

		Predicted	
		Neg.	Pos.
Actual	Neg.	TNR 78.03%	FPR 21.97%
	Pos.	FNR 21.97%	TPR 78.03%

### 5. Conclusions

This study investigated a method for estimating respiration rates which could reduce the effects that body movement has on measurements. A respiratory rate estimation system based on thresholds was developed for measuring the eCO<sub>2</sub> concentration with a wearable MOx sensor. The accuracy of the respiratory rate estimation was assessed through experimental evaluation. The results show that the developed system was able to estimate the respiration rate and was almost unaffected by body movements, achieving an accuracy of absolute error of 0.47 bpm. In this study, we found that it was possible to appropriately measure our target of 22.5 bpm. However, it is important to evaluate the developed system at not only a single frequency of 22.5 bpm but also at various frequencies. In future work, we aim to evaluate the developed system in wide ranges, such as from a single-digit bpm to 40 bpm. To expand the use of this wearable respiratory-rate-measuring device, we would like also to consider its use in daily activities like walking or running. In addition, during coughing and yawning, waveforms with frequency components similar to breathing were generated. As a result, it was confirmed that the accuracy of the estimated respiratory rate deteriorated under these conditions. For distinguishing between normal and abnormal respiration, a classification method using a one-class SVM-based approach was used and achieved 80% for the TPR and TNR. However, optimization should be performed to achieve a better performance. Future work includes expanding the experiments to include a wider range of subjects and introducing adaptive filters that dynamically eliminate the time waveforms of the eCO<sub>2</sub> concentration generated by coughing and yawning. We are also considering experimental evaluations with multiple target frequencies and want to compare the respiration rates with those using not only a metronome but also a chest belt for more accurate results. Additionally, a study on a method that could combine eCO<sub>2</sub> sensors and microphones or other wearable sensors is being considered.

**Author Contributions:** Conceptualization, M.F., D.A., T.S., R.O., T.K. and J.H.; methodology, M.F. and T.S.; software, T.S. and T.K.; validation, M.F., T.S., T.K. and R.O.; formal analysis, M.F. and T.K.; investigation, M.F., R.O. and J.H.; resources, D.A.; data curation, M.F. and R.O.; writing—original draft preparation, M.F., R.O., J.H. and D.A.; writing—review and editing, J.H., D.A. and M.F.;

visualization, M.F. and J.H.; supervision, D.A.; project administration, D.A.; funding acquisition, D.A. All authors have read and agreed to the published version of the manuscript.

**Funding:** This research was supported in part by the New Energy and Industrial Technology Development Organization (NEDO) and JSPS KAKENHI, Grant Number 24K00885.

**Institutional Review Board Statement:** The study was conducted in accordance with the Declaration of Helsinki, and approved by the Ethics Committee of Jikei University of Health Care Sciences (Ethics-ce-juhs No. 2022-1, May 2022).

**Informed Consent Statement:** Informed consent was obtained from all subjects involved in the study.

**Data Availability Statement:** The raw data supporting the conclusions of this article will be made available by the authors on request.

**Conflicts of Interest:** The authors declare no conflicts of interest.

## References

- Ishii, Y. Disasters and Respiratory Diseases (Special Feature/Disaster Medicine). *Dokkyo J. Med. Sci.* **2012**, *39*, 245–249.
- Yamauchi, K. Internal Diseases Learned from the Great Japan Earthquake—Characteristics, Response, and Prevention, Respiratory Diseases. *J. Jpn. Soc. Intern. Med.* **2014**, *103*, 551–556. [[CrossRef](#)] [[PubMed](#)]
- Uchiyama, I. Long-term Health Effects of Dust Inhalation in the Great East Japan Earthquake: Assessing Asbestos Risk. *J. Soc. Risk Anal. Jpn.* **2011**, *21*, 175–182.
- Maeda, H.; Nakagawa, M.; Yokoyama, M. Hospital admissions for respiratory diseases in the aftermath of the great Hanshin earthquake. *Jpn. J. Thorac. Dis.* **1996**, *34*, 164–173.
- Akasaka, K.; Baba, R.; Isshiki, M.; Namba, T.; Abe, K. A Proposal for a System for Real-Time Monitoring of the Health Status of Disaster Victims in Evacuation Centers. In Proceedings of the 82nd National Conference of Information Processing Society of Japan, Nonoichi, Japan, 5–7 March 2020; Volume 1, pp. 193–194.
- Shimazaki, T.; Anzai, D.; Watanabe, K.; Nakajima, A.; Fukuda, M.; Ata, S. Heat stroke prevention in hot specific occupational environment enhanced by supervised machine learning with personalized vital signs. *Sensors* **2022**, *22*, 395. [[CrossRef](#)] [[PubMed](#)]
- Furuguchi, M.; Shibata, Y.; Hashimoto, K. Emergency Physical Condition Management System Using Wearable Devices. In Proceedings of the 78th National Conference of Information Processing Society of Japan, Yokohama, Japan, 10 March 2016; pp. 987–988.
- Tamura, T. Medical Applications of Wearable Sensors and Non-Contact Sensors. *Jpn. J. Med. Instrum.* **2020**, *90*, 11–23.
- Yamaguchi, M.; Sekiguchi, K. *Development of Disease-Specific Nursing Processes*, 4th ed.; Gakken Medical Shu-Jun-Sha: Shinagawa-ku, Japan, 2013.
- Suzuki, H.; Machi, T.; Shinohara, T.; Kaito, K.; Sato, M. Impedance Method in Non-Invasive Biometry. *Jpn. Soc. Extra-Corpor. Technol. Med.* **1977**, *3*, 357–360.
- Nakajima, K.; Tamura, T.; Miike, H. Simultaneous Heart Rate and Respiration Rate Monitoring by Photoelectric Pulse Wave Method Using Digital Filter. *Jpn. J. Med. Electron. Biol. Eng.* **1993**, *31*, 360–366.
- Medical Equipment Center. *Basic Knowledge of Medical Devices*; Yakuji Nippo, Limited.: Chiyoda-ku, Japan, 2008; pp. 85–88.
- Nassar, B.S.; Schmidt, G.A. Capnography for monitoring of the critically ill patient. *Clin. Chest Med.* **2022**, *43*, 393–400. [[CrossRef](#)] [[PubMed](#)]
- Kristiansen, S.; Nikolaidis, K.; Plagemann, T.; Goebel, V.; Traaen, G.M.; Øverland, B.; Akerøy, L.; Hunt, T.E.; Loennechen, J.P.; Steinshamn, S.L.; et al. A clinical evaluation of a low-cost strain gauge respiration belt and machine learning to detect sleep apnea. *Smart Health* **2023**, *27*, 100373. [[CrossRef](#)]
- Charlton, P.H.; Birrenkott, D.A.; Bonnici, T.; Pimentel, M.A.; Johnson, A.E.; Alastruey, J.; Tarassenko, L.; Watkinson, P.J.; Beale, R.; Clifton, D.A. Breathing rate estimation from the electrocardiogram and photoplethysmogram: A review. *IEEE Rev. Biomed. Eng.* **2017**, *11*, 2–20. [[CrossRef](#)] [[PubMed](#)]
- Aqueveque, P.; Gómez, B.; Monsalve, E.; Germany, E.; Ortega-Bastidas, P.; Dubo, S.; Pino, E.J. Simple Wireless Impedance Pneumography System for Unobtrusive Sensing of Respiration. *Sensors* **2020**, *20*, 5228. [[CrossRef](#)] [[PubMed](#)]
- Romano, C.; Nicolò, A.; Innocenti, L.; Bravi, M.; Miccinilli, S.; Sterzi, S.; Sacchetti, M.; Schena, E.; Massaroni, C. Respiratory Rate Estimation during Walking and Running Using Breathing Sounds Recorded with a Microphone. *Biosensors* **2023**, *13*, 637. [[CrossRef](#)] [[PubMed](#)]
- Tarassenko, L.; Villarroel, M.; Guazzi, A.; Jorge, J.; Clifton, D.A.; Pugh, C. Non-contact video-based vital sign monitoring using ambient light and auto-regressive models. *Physiol. Meas.* **2014**, *35*, 807. [[CrossRef](#)] [[PubMed](#)]
- Singh, O.P.; Howe, T.A.; Malarvili, M.B. Real-time human respiration carbon dioxide measurement device for cardiorespiratory assessment. *J. Breath Res.* **2018**, *12*, 026003. [[CrossRef](#)] [[PubMed](#)]
- Pietraru, R.N.; Nicolae, M.; Mocanu, Ş.; Merezeanu, D.-M. Easy-to-Use MOX-Based VOC Sensors for Efficient Indoor Air Quality Monitoring. *Sensors* **2024**, *24*, 2501. [[CrossRef](#)] [[PubMed](#)]

21. Meinsberg KSI. Survey Report: Signal Processing on Metal Oxide Gas Sensors to Estimate the Indoor Carbon Dioxide Concentration on the Example IDT's ZMOD4410 Gas Sensor Module. 2018. Available online: <https://www.renesas.com/us/en/document/rep/ksi-report-review-renesas-eco2-solution-technology-evaluation> (accessed on 10 April 2024).
22. Stoukatch, S.; Fagnard, J.F.; Dupont, F.; Laurent, P.; Debliquy, M.; Redouté, J.M. Low Thermal Conductivity Adhesive as a Key Enabler for Compact, Low-Cost Packaging for Metal-Oxide Gas Sensors. *IEEE Access* **2022**, *10*, 19242–19253. [[CrossRef](#)]
23. Dutta, S.; Sivaraj, D.; Joga Rao, V.S.; Kumar, H.; Kalita, K. Development of air quality monitoring and notification system using nordic thingy IoT Kit. In Proceedings of the Industry Interactive Innovations in Science, Engineering & Technology (I3SET2K19), Kalyani, India, 13–14 December 2019.
24. Hsu, C.-W.; Lin, C.-J. A comparison of methods for multiclass support vector machines. *IEEE Trans. Neural Netw.* **2002**, *13*, 415–425. [[CrossRef](#)]
25. Tang, Y.; Fan, E.; Yan, C.; Bai, X.; Zhou, J. Discriminative weighted band selection via one-class SVM for hyperspectral imagery. In Proceedings of the 2016 IEEE International Geoscience and Remote Sensing Symposium (IGARSS), Beijing, China, 10–15 July 2016; IEEE: Piscataway, NJ, USA, 2016; pp. 2765–2768. [[CrossRef](#)]

**Disclaimer/Publisher's Note:** The statements, opinions and data contained in all publications are solely those of the individual author(s) and contributor(s) and not of MDPI and/or the editor(s). MDPI and/or the editor(s) disclaim responsibility for any injury to people or property resulting from any ideas, methods, instructions or products referred to in the content.